Chiral Biphenylacetylene Smectic Liquid Crystals

Laura de Vega,[†] Pedro D. Ortiz,[†,‡] Gunther Hennrich,[*,†] Ana Omenat,[§] Rosa M. Tejedor,[§] Joaquín Barberá,[§] Berta Gómez-Lor,[||] and José Luis Serrano[§]

Departamento de Química Orgánica, Universidad Autónoma de Madrid, Cantoblanco, 28049 Madrid, Spain, Departamento de Química Orgánica, Facultad de Ciencias-Instituto de Ciencia de Materiales de Aragón (ICMA), Universidad de Zaragoza-CSIC, Pedro Cerbuna 12, 50009 Zaragoza, Spain, and Instituto de Ciencia de Materiales de Madrid (ICMM), ICMM-CSIC, Cantoblanco, 28049 Madrid, Spain

Received: January 18, 2010; Revised Manuscript Received: March 9, 2010

Standard Sonogashira coupling afforded rod-like, phenylacetylene extended biphenyl mesogens substituted with different chiral alkoxy chains, starting from commercially available 4-(4′-bromophenyl)phenol. Depending on the position of the chiral center and the polar nature of the target molecules as determined by the electron withdrawing end-groups, different types of smectic liquid crystals are formed. The liquid crystal phases are fully characterized by polarized optical microscopy, differential scanning calorimetry, and X-ray diffraction. In two cases, the molecular chirality is transferred to the supramolecular assembly, which is proved by circular dichroism measurements in the chiral mesophase.

1. Introduction

In smectic liquid crystal (LC) phases, the molecules present orientational and at least short-range translational order within a layered structure. In the smectic A phase, the long axis of the rod-like (calamitic) mesogens is on average perpendicular to the layer. Depending on the strength of the molecular dipole moment, the calamitics are inclined to arrange in an antiparallel fashion, forming bilayers as a consequence. In the smectic C phase, the molecular axis of the mesogens is tilted with respect to the layer normal. The orientation of the molecules responds to an external electric field which is the basis of conventional LC applications, primarily in display technology.[1] The formation of chiral smectic LC phases is the result of an ordered, layer by layer propagation of the tilt angle in a way that the ensemble of the molecular units adopts the aforementioned helical arrangement on the macroscopic level.[2] Since the early reports on ferroelectric LCs more than three decades ago, substantial research effort dedicated to chiral LC systems persists.[3] As a consequence of the presence of a stereocenter in the molecular unit, the mesogens can adopt a helical conformation in the bulk. Thus, the chirality on the molecular level is transferred on the macroscopic scale in the LC phase, leading to interesting applications in advanced display, sensing, and nonlinear optical devices.[4] No general rules exist which directly predict the magnitude and sense of helical twisting in the superstructure as the consequence of the position and absolute configuration of the mesogenic unit. This is why one has to rely on the extrapolation of established structure−activity relationships as guidelines for the design of new supramolecular materials. Here, we present the synthesis of novel chiral biphenylacetylene LCs and study their mesomorphic and chiroptical properties. The elongation of the biphenyl core by *p*-phenylethynyl units yields molecular scaffolds which hold great promise as advanced electro-optical and high-birefringent materials.[5] Sonogashira coupling is the methodology of choice in order to obtain alkynyl-expanded biphenyls.[6] Different chiral alkyl chains are introduced at the phenyl or biphenyl units as terminal substituents, and the position and nature of the chiral substituent on the chirality of the resulting LC phases is evaluated.

2. Results and Discussion

2.1. Synthesis. Commercially available 4-bromo-4′-hydroxybiphenyl was first alkylated with the respective bromoalkanes to give bromobiphenyls **1a** and **2a** and then subjected to a standard coupling-deprotection procedure to give the ethynylbiphenyls **1**[7] and **2** as key intermediates (Scheme 1).

The target compounds **3**−**5** are obtained in a second coupling step with corresponding substituted iodobenzenes in good yields (Scheme 2). To our surprise, the supposedly straightforward Sonogashira coupling of commercially available *p*-ethynylbenzene derivatives with the bromobiphenyls **1a** and **2a** did not give the desired products.

The synthesis of alkynylbiphenyl **6** with the chiral alkyl chain situated at the biphenyl terminus is initiated by the modification of the commercial biphenyl precursor: 4-(4′-Bromophenyl)acetophenone is oxidized by *tert*-butyl hydroperoxide (TBHP) in alkaline aqueous solution, catalyzed by WO_3,[8] to give 4′-bromobiphenyl-4-carboxylic acid.[9] After esterification of the carboxylic acid with (*S*)-(−)-2-methyl-1-butanol, the ethynyl group is introduced using a standard protocol, i.e., Pd-catalyzed coupling of trimethylsilylacetylene (TMSA) followed by basic cleavage of the TMS protecting group, yielding **6b**.[10] A second Sonogashira coupling step employing 1-decyloxy-4-iodobenzene[11] gives compound **6** as the final product (Scheme 3).

2.2. Experimental Section. All compounds are fully characterized by ^{1}H and ^{13}C NMR spectra, elemental analysis, and mass spectrometry. Full synthetic experimental procedures and characterization of the target compounds are included in the Supporting Information.

Techniques. The optical textures of the mesophases were studied with an Olympus polarizing microscope BX51 equipped with a Linkam hot-stage and Linkam TMS 91 central processor.

* To whom correspondence should be addressed. E-mail: gunther.hennrich@uam.es.
† Universidad Autónoma de Madrid.
‡ Present address: Departamento de Química Inorgánica, Universidad de La Habana, La Habana 10400, Cuba.
§ Universidad de Zaragoza-CSIC.
|| ICMM-CSIC.

10.1021/jp1004727
Published on Web 03/25/2010

SCHEME 1: Synthesis of Ethynylbiphenyls 1 and 2

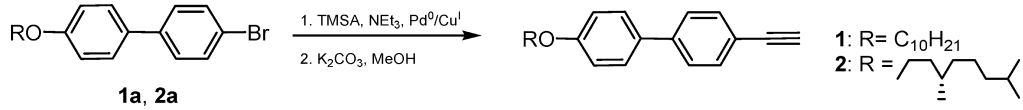

SCHEME 2: Synthesis of Alkynylbiphenyls 3−5

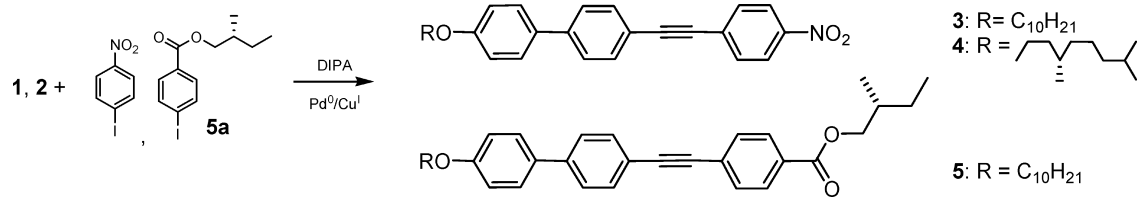

SCHEME 3: Synthesis of Alkynylbiphenyl 6

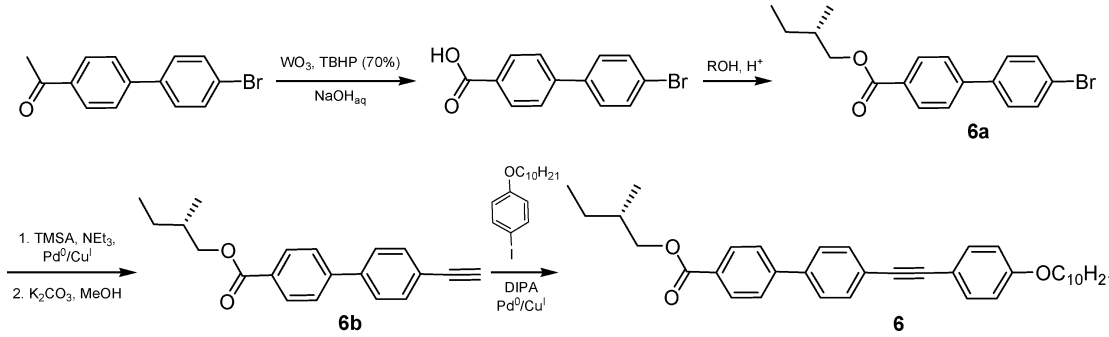

The transition temperatures and enthalpies were measured by differential scanning calorimetry with a TA Instruments Q20 instrument operated at a scanning rate of 10 °C min^{-1} on both heating and cooling. The apparatus was calibrated with indium (156.6 °C; 28.4 J g^{1-}) as the standard. The XRD patterns were obtained with a pinhole camera (Anton-Paar) operating with a point-focused Ni-filtered Cu Kα beam. The sample was held in Lindemann glass capillaries (1 mm diameter) and heated, when necessary, with a variable-temperature oven. The capillary axis is perpendicular to the X-ray beam, and the pattern is collected on flat photographic film perpendicular to the X-ray beam. Spacings were obtained via Bragg's law. UV−vis and CD spectra of acetonitrile solution (around 10^{-5} M) and a thin film of synthesized compounds were registered simultaneously using a Jasco J-810 spectropolarimeter. Films were prepared by casting solutions of the materials in dichloromethane onto clean, fused silica slides and heated to the isotropic temperature for 5 min and then sited on a metal block at 25 °C for 5 min. Then, the films were placed in a rotating holder around the light beam axis with temperature control. The CD spectra of the films were registered both in a heating run starting at 5 °C above melting temperature and measured every 5 °C up to the isotropization temperature, and afterward in the cooling process until the crystallization of the sample occurs. In all of the cases, the negligible contribution of linear dichroism was confirmed comparing the CD spectra registered rotating the sample every 60° around the light beam axis.

2.3. Mesomorphic Behavior. The thermal properties of the biphenylacetylenes **3**−**6** were studied by differential scanning calorimetry. Phase transition temperatures and the corresponding enthalpy values were collected from the second heating scans. The mesophases were identified by the observation of their textures by polarized optical microscopy (POM),[12] and by X-ray diffraction. The data is summarized in Tables 1 and 2.

Biphenylacetylenes **3** and **4** display comparable phase behavior where an ordered lamellar structure, which we have named as ordered Sm in Tables 1 and 2, is followed by the appearance of a SmA phase. The ordered character of the low-temperature mesophase is revealed by the existence of a number of sharp maxima at high diffraction angles in addition to a set of equally spaced maxima at low angles. The comparison of the experimental values obtained for the layer spacings and the estimated molecule length using molecular modeling allows us to deduce that the SmA phase presents a partially interdigitated bilayer structure, which is usually found for mesogens with highly polar groups, such as nitro or cyano.[13,14] This phenomenon is accounted for by the antiparallel arrangement of the mesogens. The symmetry of the orthogonal SmA phase prevents the formation of a helical structure when introducing chirality in the molecules forming the mesophase. However, compounds **5** and **6** exhibit tilted mesophases (hexatic I or F and C in the case of **5** and C for **6**), in which the molecules form a helical organization in the mesophase when chiral centers are present in the molecular structure. The exact nature (I or F) of the hexatic mesophase cannot be determined on the basis of the X-ray diffraction only. Table 2 gathers the layer thickness measured by X-ray diffraction at variable temperatures for the smectic mesophases of compounds **5** and **6**. It is noteworthy

TABLE 1: LC Phases[a] and Transition Properties for Compounds 3−6

compound	transition temperatures (°C) and enthalpies (ΔH/kJ mol^{-1})
3	Cr 93.9 (28.4) ordered Sm 172.5 (6.8) SmA 216.5 (2.3) I
4	Cr 76.3 (2.6) ordered Sm 166.5 (7.7) SmA 228.5 (7.7) I
5	Cr 64.2 (4.0) Cr′ 119.8 (1.5) hexatic Sm* 136.6 (2.9) SmC* 158.4 (0.4) SmA 189.8 (4.2) I
6	Cr 122.5 (4.9) SmC* 147.2 (0.4) SmA 182.4 (3.7) I

[a] Cr, crystal; ordered Sm, ordered smectic phase; SmA, smectic A; hexatic Sm*, chiral hexatic tilted (I or F); SmC*, chiral smectic C; I, isotropic liquid.

TABLE 2: X-ray Diffraction Data for Compounds 3−6

compound	T (°C)	phase	d-layer thickness (Å)	tilt angle ($\cos^{-1} d_C/d_A$)	L^a (Å)
3	100	ordered Sm	34.4		32
	175	ordered Sm	34.7		
	185	SmA	36.5		
	195	SmA	37.3		
4	r.t.	crystal			30
	175	ordered Sm	35.1		
	185	SmA	35.8		
	190	SmA	35.8		
					38
5	90	crystal			
	105	crystal			
	125	hexatic Sm*	31.9		
	145	SmC*	31.8	27°	
	165	SmA	34.0		
	185	SmA	35.7		
6	r.t.	crystal			38
	90	crystal′			
	135	SmC*	31.3	29°	
	155	SmA	35.7		
	175	SmA	35.7		

[a] *L*: Estimated molecule length using Dreiding stereomodels assuming a fully extended conformation of the hydrocarbon chains.

that the *d*-layer thickness of the SmA mesophase measured for compound **5** is significantly temperature dependent. At 165 °C, the *d*-layer thickness is 34.0 Å, whereas, at 185 °C, this value increases to 35.7 Å. This indicates that the molecules are tilted to a certain extent even in the low-temperature range of the SmA mesophase. Such a difference in the *d*-layer spacing is not observed in the case of compound **6,** for which the values measured at 155 and 175 °C are the same, although if the experimental error of the measurement (±0.5 Å) is considered, a certain tilt of the molecules in the SmA mesophase might exist. The circular dichroism (CD) experiments performed on these compounds confirm the results obtained by XRD (see below). Comparing the SmC* and SmA layer spacings, the tilt angle of the molecules in the SmC* mesophase can be calculated as $\theta = \cos^{-1} d_C/d_A$, with d_C and d_A being the layer thickness in the SmC and SmA phases. The results of these calculations are 27 and 29° for **5** and **6**, respectively. Moreover, the layer thickness measured for the SmA mesophase of **5** and **6** indicates that, in these cases, a monolayer structure is formed which is expected to be due to the presence of only weakly polar ester groups as terminal substituents of the mesogenic unit. Although theoretically the layer spacing measured in the higher temperature range of the smectic A mesophase of these compounds would be expected to be equal to the molecular length, the value obtained experimentally is smaller than the one predicted from molecular models. This phenomenon, very common in liquid crystals, is due to the conformational freedom of the hydrocarbon chains in the mesophase (presence of a number of *gauche* bonds), as well as to the possibility of local fluctuations of the direction of the molecular axes, all of which can reduce the effective length. For compounds **5** and **6**, the measured layer spacing *d* is smaller by 2−2.5 Å than the molecule length *L* (Table 2). It is interesting to note that the tilt angle could also be deduced as $\theta = \cos^{-1} d/L$. By using this formula, it is assumed that, in the mesophase, the molecules are in their most extended conformation, i.e., with their hydrocarbon chains in the *all-anti* arrangement. However, as mentioned above, this is not the case for the SmA mesophase of compounds **5** and **6**. It can be safely deduced that in the SmC* mesophase the molecules do not adopt a fully extended conformation and thus the actual molecule length is smaller than *L* and much closer to the layer spacing *d* measured in the high temperature range of the SmA mesophase. Therefore, the tilt angles calculated with the formula $\theta = \cos^{-1} d_C/d_A$ are more realistic and, obviously, they are smaller than those calculated with the formula based on the assumption of fully extended molecules.

The circular dichroism (CD) experiments performed on these compounds confirm the results obtained by XRD (see below). Comparing the SmC* and SmA layer spacings, the tilt angle of the molecules in the SmC* mesophase can be calculated, resulting in 27 and 29° for **5** and **6**, respectively. Moreover, the layer thickness measured for the SmA mesophase of **5** and **6** indicates that, in these cases, a monolayer structure is formed which is expected to be due to the presence of only weakly polar ester groups as terminal substituents of the mesogenic unit. The transitions from the SmA to the chiral Sm* phases (SmC* and hexactic Sm*) result in layer contractions substantially bigger than those defined for a "de Vries-like" behavior (≤1%).[1a,15]

TABLE 3: Calculated Dipole Moments for 4−6

compound	μ (D)	σ_p[19]
4	8.07	NO_2: 0.78
5	3.01	CO_2CH_3: 0.45
6	3.21	CO_2CH_3: 0.45

2.4. Electro-optical Characterization. A 5 μm thick Linkam LC cell was filled with compound **5** in the isotropic liquid phase. Unfortunately, it was not possible to obtain a well-oriented sample by slow cooling of the cell and/or by applying an electric field. Electro-optical switching was observed in the temperature intervals corresponding to both ferroelectric mesophases, SmC* and hexatic Sm*, by the application of an electric field (triangular wave, 50 Vp-p, 1 Hz frequency).[16] However, the determination of the spontaneous polarization of compound **5** in these mesophases was not possible in our experimental setup.

To elucidate the differences in the mesomorphic behavior, computational calculations (DFT//B3LYP/6-311G[d,p]) have been performed to assess the molecular dipole moment μ of **4**, **5**, and **6**. For simplification, the alkyl substituents in the ether or ester groups are calculated as methyl groups. Table 3 summarizes the calculated dipole moments for the biphenylacetylenes **4**−**6** depending on the electronegativity on the terminal phenyl units as defined by Hammet substituent constants σ_p.[17] It is straightforward that the high dipole moment of 8.07 D for **4** is responsible for the high order in the SmA phase and the for the formation of bilayers in the LC phase. We attribute the distinct mesomorphism of **5** vs **6** to subtle differences in the dipole moments of both, which in consequence affects the alignment of the molecules in the bulk. On the molecular level, this variation stems from the less efficient π-conjugation in the biphenyl fragment of **5**.[18]

2.5. Circular Dichroism. An expected result for the achiral biphenylacetylene compound **3** is that its acetonitrile solution is CD-silent. Under the chosen experimental conditions, acetonitrile solutions of chiral compounds **4**, **5**, and **6** do not exhibit CD responses either (i.e., the expected signal is below the detection limit). Subsequently, in solution, no intrinsic CD due to molecular chirality is detected in the UV−vis range, as the chiral centers do not exhibit absorption bands in this spectral range. Moreover, these chiral groups do not exert symmetry-breaking perturbation of the electronic states of the chromophores (Figures S1 and S2, Supporting Information). In order to study the progress of the induced CD with the temperature

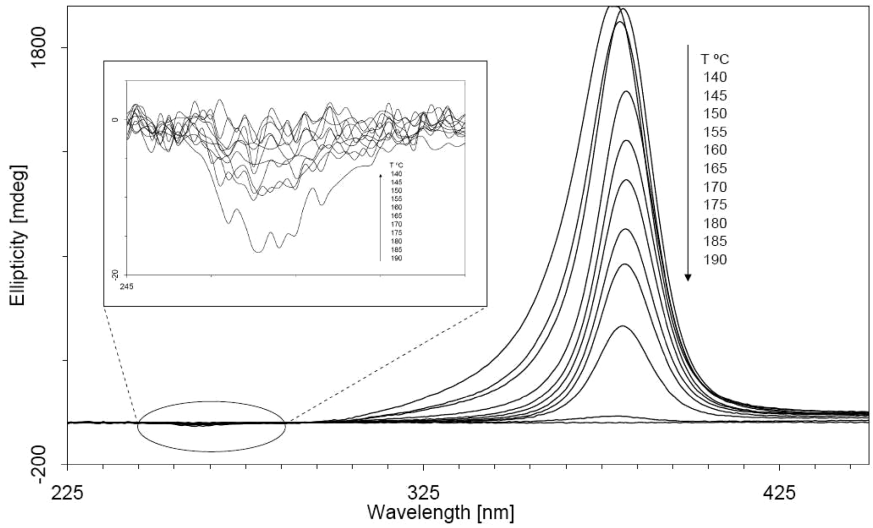

Figure 1. CD spectra of **5** from 140 to 190 °C, registered every 5 °C. Inset: CD spectra in the 245−285 nm range from 140 to 190 °C, registered every 5 °C.

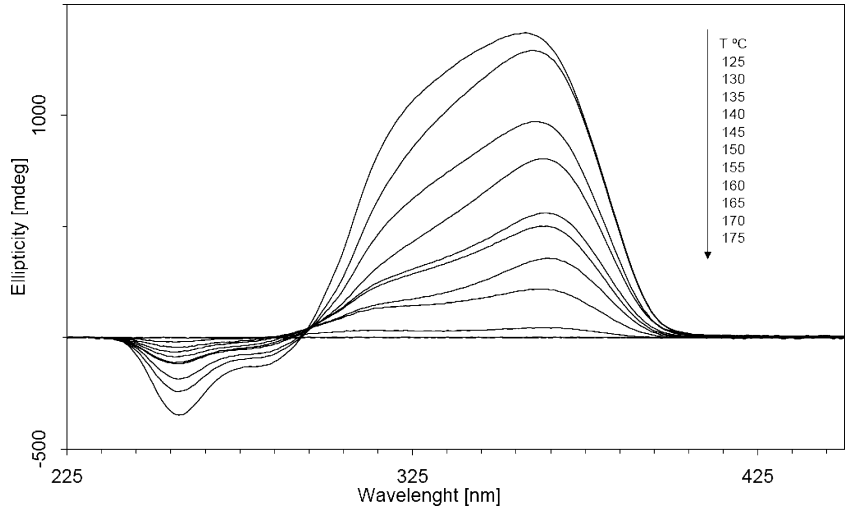

Figure 2. CD spectra of **6** from 125 to 175 °C registered each 5 °C.

and liquid crystal order, the CD spectra of the chiral compounds which exhibit helical mesophases, **5** and **6**, were registered within the mesogenic range every 5 °C on heating. These results are displayed in Figures 1 and 2, respectively. CD spectra of **5** for the hexatic Sm* temperature range (125−135 °C) are included in the Supporting Information (Figure S3).

The chiral organization of a helical liquid crystal mesophase induces significant CD responses. In fact, chiral compounds **5** and **6** display intense CD signals in the helical mesophases (hexatic Sm* and SmC*) and, surprisingly, also in the orthogonal mesophase (SmA*). On the other hand, the achiral mesophase of chiral compound **4** is CD silent. The CD spectra of compounds **5** and **6** show two Cotton effects of opposite sign. Both of them exhibit a negative Cotton effect at shorter wavelengths and a positive one at longer wavelengths. These bands are attributed to the transition whose moments are perpendicular and parallel to the molecular long axis, respectively.[20] Figures 3 (**5**) and 4 (**6**) show the temperature dependence of the CD signal at the maximum of the positive Cotton effect relative to the ellipticity value at the beginning of the SmC* phase (140 °C for **5** and 125 °C for **6**).

As a result of the liquid crystalline order, the CD signal varies with the temperature and no discontinuity exists at the SmC* and SmA* phase transition. In addition, the SmA* phases exhibit

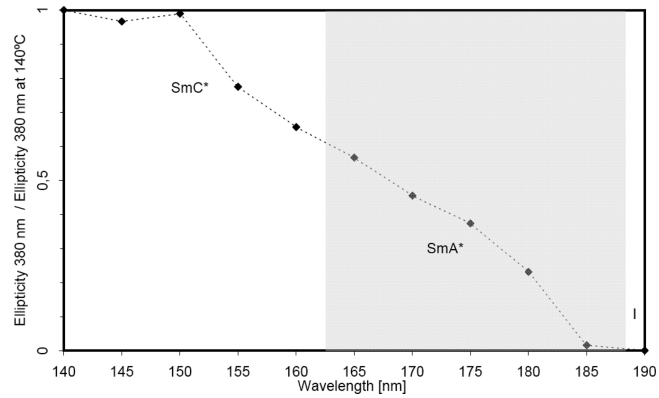

Figure 3. Temperature dependence of the CD of **5** at the maximum of the positive Cotton effect relative to the ellipticity value at 140 °C.

CD responses and the sign of the CD signal in the SmA* phase is always the same as that in the SmC* phase. Similar results are obtained in the cooling scan. These results indicate the existence of some helical structures in the SmA* phases, and consequently, the molecular tilt is not zero.[2] In fact, X-ray diffraction data supports these results as stated above.

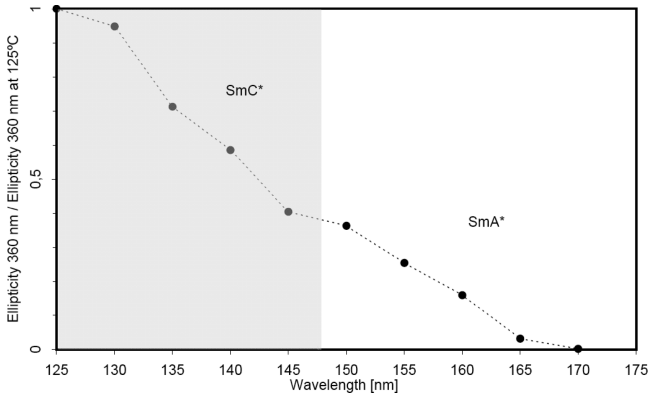

Figure 4. Temperature dependence of the CD of **6** at the maximum of the positive Cotton effect relative to the ellipticity value at 125 °C.

3. Conclusion

Straightforward synthetic protocols are presented for accessing various acetylenic biphenyl derivatives from commercially available biphenyl precursors. Chiral alkyl chains can be placed on the phenylethynyl and biphenyl terminus, likewise. Highly polar π-systems are obtained by incorporating a terminal NO_2 substituent. As a consequence, the mesogens arrange in an antiparallel fashion, forming bilayers, and the molecular chirality of **4** brought about by the terminal alkyl chain is canceled out by the high supramolecular order in the bulk. In contrast, the moderately polar ester derivatives **5** and **6** form chiral LC phases; i.e., the molecular chirality is efficiently transferred to the supramolecular level. In their chiral smectic (SmC*) phases, the calamitics are considerably tilted, and especially biphenylacetylene **5** displays a rich polymorphism. The differences in their phase behavior are simply the result of the positioning of the chiral center along the biphenylacetylene system, which would have been impossible to predict *ab initio*. More than simply giving insight into the structure−activity relationship, which is useful for the design of LC materials, both compounds display intriguing chiroptical properties potentially useful in optic and photonic applications.

Acknowledgment. We thank the CCC of the UAM and the following institution for financial support: MEC (Spain), grants CTQ2007-65683, CTQ2006-15611-CO2-01, and MAT2008-06522-C02.

Supporting Information Available: General methods, full synthetic procedures, and compound characterization for **2a**−**6**; POM images for **3**−**6**; UV−vis and CD spectra of **3**, **4**, **5**, and **6** in acetonitrile; CD spectra of **5** in the hexatic Sm* phase; and computational modeling. This material is available free of charge via the Internet at http://pubs.acs.org.

References and Notes

(1) (a) Demus, D.; Goodby, J.; Gray, G. W.; Spiess, H.-W.; Vill, H.-W.; Lagerwall, S. T. *Handbook of Liquid Crystals*; Wiley-VCH: Weinheim, Germany, 1998; Vol. 2B, Chapter VI 2, pp 515−664. (b) Collings, P. J. *Liquid Crystals: Nature's Delicate Phase of Matter*; Princeton University Press: Princeton, NJ, 1990.

(2) (a) Goodby, J. W.; Saez, I. M.; Cowling, S. J.; Görtz, V.; Draper, M.; Hall, A. W.; Sia, S.; Cosquer, G.; Lee, S.-E.; Raynes, E. P. *Angew. Chem., Int. Ed.* **2008**, *17*, 2754–2787. (b) Lagerwall, J. P. F.; Giesselmann, F. *ChemPhysChem* **2006**, *7*, 20–45.

(3) (a) Lemieux, R. P. *Chem. Soc. Rev.* **2007**, *36*, 2033–2045. (b) Lemieux, R. P. *Acc. Chem. Res.* **2001**, *34*, 845–853. (c) Goodby, J. W. *Science* **1986**, *321*, 350–355.

(4) (a) Ha, N. Y.; Jeong, S. M.; Nishimura, S.; Suzaki, G.; Takanishi, Y.; Ishikawa, K.; Takezoe, H. *Nat. Mater.* **2008**, *7*, 43–47. (b) Chen, H. M.; Katsis, D.; Chen, S. H. *Chem. Mater.* **2003**, *15*, 2534–2542. (c) Walba, D. M.; Eshdat, L.; Korblova, E.; Shao, S.; Clark, N. A. *Angew. Chem., Int. Ed.* **2007**, *46*, 1473–1475. (d) Yamane, S.; Sagara, Y.; Kato, T. *Chem. Commun.* **2009**, 3597–3599. Walba, D. M.; Dyer, D. J.; Sierra, T.; Cobben, P. L.; Shao, R.; Clark, N. A. *J. Am. Soc.* **1996**, *118*, 1211–1212.

(5) O'Neil, M.; Kelly, S. M. *Adv. Mater.* **2003**, *15*, 1135–1146.

(6) (a) Tykwinski, R. R. *Angew. Chem., Int. Ed.* **2003**, *42*, 1566–1568. (b) Chinchilla, R.; Nájera, C. *Chem. Rev.* **2007**, *107*, 874–922.

(7) Ely, F.; Conte, G.; Merlo, A. A.; Gallardo, H. *Liq. Cryst.* **2004**, *31*, 1413–1425.

(8) Shaikh, T. M. A.; Sudalai, A. *Eur. J. Org. Chem.* **2008**, 4877–4880.

(9) Dolman, S. J.; Gosselin, F.; O'Shea, P. D.; Davies, I. W. *Tetrahedron* **2006**, *62*, 5092–5098.

(10) During the deprotection in methanol, partial transesterification is observed.

(11) Lee, S. J.; Park, C. R.; Chang, J. Y. *Langmuir* **2004**, *20*, 9513–9519.

(12) Dierking, I. *Textures of Liquid Crystals*; Wiley-VCH: Weinheim, Germany, 2003.

(13) See the Supporting Information.

(14) Lansac, Y.; Glaser, M. A.; Clark, N. A. *Phys. Rev. E* **2001**, *64*, 051703.

(15) Roberts, J. C.; Kapernaum, N.; Song, Q.; Nonnenmacher, D.; Ayub, K.; Giesselmann, F.; Lemieux, R. P. *J. Am. Chem. Soc.* **2010**, *132*, 364–370.

(16) Naber, R. C. G.; Asadi, K.; Blom, P. W. M.; de Leeuw, D. M.; de Boer, B. *Adv. Mater.* **2010**, *22*, 933–945.

(17) Hansch, C.; Leo, A.; Taft, R. W. *Chem. Rev.* **1991**, *91*, 165–195.

(18) (a) Mank, D.; Raytchev, M.; Amthor, S.; Lambert, C.; Fiebig, T. *Chem. Phys. Lett.* **2003**, *376*, 201–206. (b) Hennrich, G.; Ortiz, P. D.; Cavero, E.; Hanes, R. E.; Serrano, J. L. *Eur. J. Org. Chem.* **2008**, 4575–4579.

(19) Ortiz, P. D.; Suardiaz, R.; de Vega, L.; Hennrich, G.; Ortiz, P. J. *J. Phys. Chem. A* **2010**, *114*, 2939–2944.

(20) Li, J.; Takezoe, H.; Fukuda, A.; Watanabe, J. *Liq. Cryst.* **1995**, *18*, 239–250.

JP1004727